

Coherent and incoherent magnons induced by strong ultrafast demagnetization in thin permalloy films

Anulekha De¹, Akira Lentfert¹, Laura Scheuer¹, Benjamin Stadtmüller^{1,2}, Georg von Freymann^{1,3}, Martin Aeschlimann¹, and Philipp Pirro¹,

¹Fachbereich Physik and Landesforschungszentrum OPTIMAS, Rheinland-Pfälzische Technische Universität Kaiserslautern-Landau, 67663 Kaiserslautern, Germany

²Institute of Physics, Johannes Gutenberg University Mainz, 55128 Mainz, Germany

³Fraunhofer Institute for Industrial Mathematics, 67663 Kaiserslautern, Germany

Understanding spin dynamics on femto- and picosecond timescales offers new opportunities for faster and more efficient devices. Here, we experimentally investigate coherent spin dynamics following ultrafast all-optical excited demagnetization measured by time-resolved magneto optical Kerr effect (TR-MOKE) in ultrathin $\text{Ni}_{80}\text{Fe}_{20}$ films. On nanosecond time scales, we provide a detailed investigation of the magnetic field and pump fluence dependence of the GHz frequency precessional dynamics. We discuss how the unusual dependence of the lifetime of the coherent precession can be related to the dephasing due to nonlinear magnon interactions and the incoherent magnon background.

Index Terms—

I. INTRODUCTION

THE laser-induced magnetization dynamics in femto-, pico- and nanosecond time-scales has created a new paradigm in condensed matter physics. Using the time-resolved magneto-optical Kerr effect (TR-MOKE), one can directly address the processes responsible for the excitation and relaxation of a magnetic system on their characteristic timescales [1], [2]. The pioneering work by Beaurepaire et al. in 1996 on femtosecond laser induced ultrafast demagnetization opened up a new avenue toward the ultrafast manipulation of magnetization in magnetic materials [3]. Only a few years later, experiments could show that the used ultrafast laser pulses also create coherent magnons, manifested as precessional dynamics on the nanosecond time scale. This precessional regime allows to study the magnetic anisotropy, damping, and precession frequency of different dynamic modes in continuous thin films and patterned nanostructures [2], [4], [5]. For example, van Kampen, et al. [1] demonstrated using TR-MOKE that an optical pump pulse can create coherent uniform spin precession in a ferromagnet. The excitation of these magnons was explained by a thermally altered magnetic anisotropy. Later, several works were concerned with exploring the precessional relaxation mechanisms in ferromagnets after ultrafast excitation [5]–[9].

In this article, we take a closer look at the relaxation of the coherent precession induced by ultrafast demagnetization and study in detail the decay time of the measured coherent oscillations as a function of magnetic field and pump fluence. We use femtosecond amplified laser pulses for excitation and detection of the magnetization dynamics in ultrathin Py films including ultrafast demagnetization, fast and slow remagnetization and precessional dynamics. We observe a magnetic field dependence of the precessional lifetime which is not in accordance with the expectations from the Gilbert model. We relate this observation to the dephasing associated with

nonlinear magnon interactions and the variable contribution of the incoherent magnon background after excitation by a fs laser pulse.

II. MATERIALS AND METHODS

Permalloy ($\text{Ni}_{80}\text{Fe}_{20}$, Py) films of 5 nm and 2.8 nm thickness have been deposited on MgO substrates by molecular beam epitaxy (MBE) technique in an ultrahigh vacuum chamber. Prior to the deposition of the metal layers, an additional epitaxial MgO buffer layer was deposited. On this substrate, Py layers with thicknesses of 2.8 nm and 5 nm are grown. Finally, the samples were capped with 3 nm thick Al_2O_3 to protect the sample surface from environmental degradation, oxidation and laser ablation during the pump-probe experiment using femtosecond laser pulses.

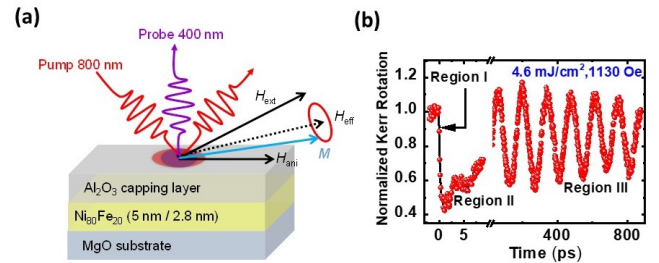


Fig. 1. (a) Schematic diagram of the measurement geometry. (b) Typical experimental TR-MOKE data showing different temporal regimes of the magnetization dynamics for 5 nm Py sample measured at $\mu_0 H = 113$ mT and $F = 4.6$ mJ cm⁻².

We have inspected the magnetization dynamics by a time-resolved magneto optical Kerr effect (TR-MOKE) set up based on two-color, non-collinear optical pump-probe technique. In this experiment, we use the fundamental output of an amplified femtosecond laser system with wavelength (λ) of 800 nm,

repetition rate of 1 kHz, and pulse width of ~ 35 fs (Libra, Coherent Inc.) to pump the magnetization, whereas, its second harmonic ($\lambda = 400$ nm) is used to probe the dynamics. The probe is normally incident onto the sample, while the pump is incident obliquely ($\sim 30^\circ$ with the surface normal). During the measurements, we have applied a magnetic field inclined at a small angle of $\sim 15^\circ$ to the sample plane. The inclination of magnetization provides a finite out-of-plane demagnetizing field which is modified using the pump pulse to induce the precession of magnetization [10]. This symmetry break is important to obtain the same starting phase of the precessional motion for every laser pump pulse to avoid that the precessional signal is lost in the averaging process performed in the TR-MOKE experiments. To obtain the intrinsic magnetic response, we have performed the measurements for two opposite direction of magnetization of the sample and extract the pure magnetic response from the difference of the two resulting signals. This is done in order to preclude any nonmagnetic signal, i.e., any signal that does not depend of the direction of the sample magnetization [11]. We have used a specially designed photodetector connected to a lock-in amplifier to measure the dynamic Kerr rotation signal. All measurements have been performed under ambient condition and room temperature. A schematic diagram of the measurement geometry is shown in Fig. 1(b).

III. RESULTS AND DISCUSSION

A. Laser induced ultrafast demagnetization

Several processes occur when a femtosecond laser pulse interacts with a ferromagnetic thin film in its saturation condition. First of all, the magnetization of the system is partially or fully lost within hundreds of femtoseconds, which is known as ultrafast demagnetization [3]. This is generally followed by a fast recovery of the magnetization within sub-picoseconds to a few picoseconds and a slower recovery within hundreds of picoseconds, known as the fast and slow remagnetizations. The slower recovery is accompanied by a magnetization precession. On a much longer timescale of a few nanoseconds, the magnetization returns to its initial equilibrium, which can be phenomenologically described by the the Gilbert damping [12].

First, we study the ultrafast demagnetization and fast remagnetization processes to quantify their dependence on pump laser fluence for the system under investigation. Figure 2(a) and (b) shows the ultrafast demagnetization traces obtained for 5 nm Py in polar and longitudinal MOKE geometry respectively. The pump fluence is varied between $4.6 - 8.4$ mJ cm^{-2} by varying the power of the pump pulse. We restrict ourselves to the low fluence regime to avoid nonlinear effects and sample damage. For all our experiments, the probe fluence is kept constant at a very low value (\sim few μW) to prevent additional contribution to the spin dynamics by probe excitation. The ultrafast demagnetization traces for both the geometries exhibit qualitatively similar trends. The amplitude of the maximum quenching of the Kerr rotation signal increases with the laser fluence, allowing us to rule out nonlinear effects [13]. Closer inspection of the traces also

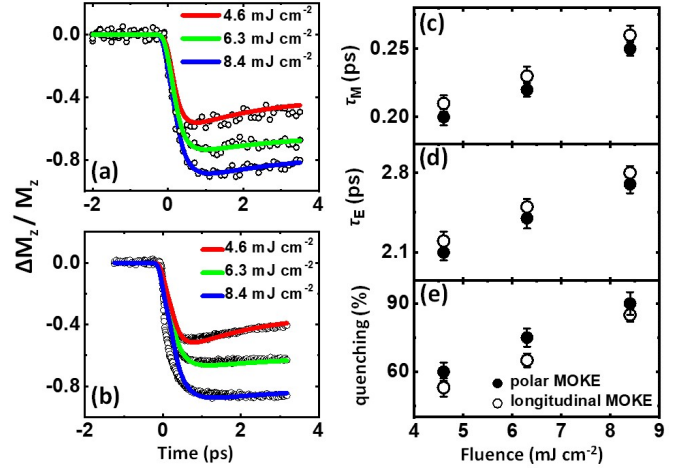


Fig. 2. Ultrafast demagnetization traces at different pump fluences for 5 nm Py sample in (a) polar (b) longitudinal MOKE geometry. (c) Demagnetization times (τ_M) vs. pump fluence (d) Fast remagnetization times (τ_E) vs. pump fluence and (e) quenching vs. pump fluence measured in both polar and longitudinal MOKE. Solid circles and open circles represent the data corresponding to polar and longitudinal MOKE respectively.

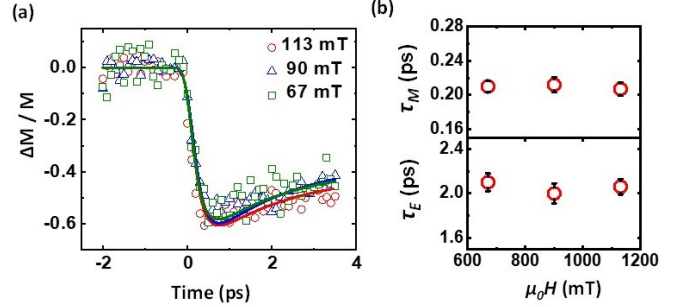


Fig. 3. (a) Ultrafast demagnetization traces for 5 nm Py sample measured at different values of H and for fixed $F = 4.6$ mJ cm^{-2} . (b) upper panel: Demagnetization times (τ_M) vs. H , lower panel: Fast remagnetization times (τ_E) vs. H .

reveals an increase of demagnetization times with increasing fluence. To quantify this increase, we fit our demagnetization traces with a phenomenological thermodynamic model, called the three-temperature model (3TM) [14],

$$-\frac{\Delta M}{M} = \left[\left(\frac{A_1}{\sqrt{1+t/\tau_0}} - \frac{A_2\tau_E - A_1\tau_M}{\tau_E - \tau_M} e^{-t/\tau_M} - \frac{\tau_E(A_1 - A_2)}{\tau_E - \tau_M} e^{-t/\tau_E} \right) H_S(t) + A_3\delta(t) \right] \otimes G(t), \quad (1)$$

which is obtained by solving the energy rate equation between three different degrees of freedom, e.g., electron, spin, and lattice under low pump fluence conditions. Here, τ_M and τ_E are ultrafast demagnetization and first relaxation times respectively. A_1 represents the amplitude of magnetization after equilibrium between the electron, spin, and lattice is restored, A_2 is proportional to the maximum rise in the electronic temperature, and A_3 represents the state filling effects during pump-probe temporal overlap described by a

Dirac delta function. $H_S(t)$ is the Heaviside step function, $\delta(t)$ is the Dirac delta distribution, and $G(t)$ is a Gaussian function that corresponds to the laser pulse. τ_0 is a constant. The demagnetization time (τ_M), fast remagnetization time (τ_E) and quenching increases with increasing pump fluence in both polar and longitudinal geometry as shown in Fig. 2 (c) – (e). These fluence-dependent behaviour of τ_M , τ_E and quenching is a hint of spin-flip process-dominated ultrafast demagnetization in our systems [15]–[17]. The values of τ_M extracted from our experiments lie in the same time scale with previous reports [18], and are too large to represent a superdiffusive transport-driven demagnetization [19]. However, τ_M , τ_E and quenching do not vary significantly with magnetic field (see Fig. 3) indicating that, as expected, the comparably small variations of the Zeeman energy as well as the small change of the magnetization direction associated with the change of the magnetic field strength do not influence the ultrafast demagnetization.

B. Precessional dynamics

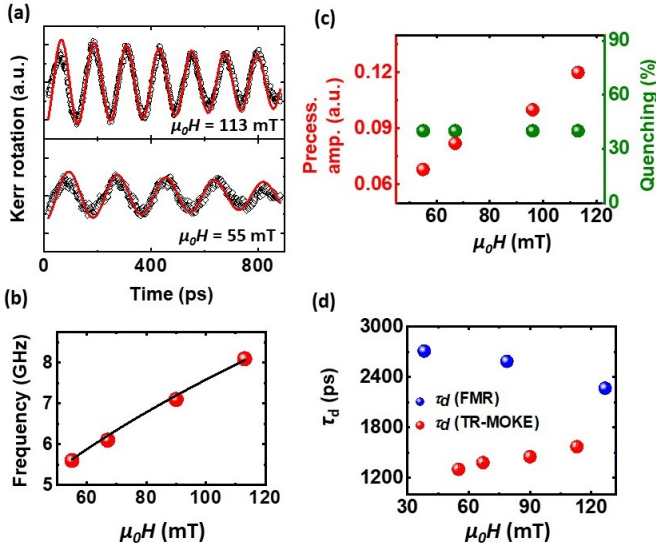


Fig. 4. Magnetic field dependent dynamics: (a) Background-subtracted time-resolved Kerr rotation data for 5 nm Py sample measured at two different magnetic fields and at $F = 4.6 \text{ mJ cm}^{-2}$. Solid lines are fitting lines. (b) Magnetic field dependence of precession frequency. Solid line represent the Kittel fit to the data points. (c) Magnetic field dependence of percentage quenching (green) and of precessional amplitude (red). (e) Magnetic field dependence of the precessional relaxation time (τ_d) measured after ultrafast demagnetization (red dots) and using microwave spectroscopy (blue dots).

After the quantification of the ultrafast demagnetization, we turn to the precessional magnetization dynamics induced by the latter. This dynamics is described by the phenomenological LLG equation [12],

$$\frac{d\vec{M}}{dt} = -\gamma\vec{M} \times \left[\vec{H}_{\text{eff}} - \frac{\alpha}{\gamma M_S} \frac{d\vec{M}}{dt} \right] \quad (2)$$

where γ is the gyromagnetic ratio, M_S is the saturation magnetization, α is the Gilbert damping constant, and H_{eff} is the effective magnetic field consisting of several field components. The first term on the right-hand of Eq. (2) accounts for

the precession of the magnetization vector (\vec{M}) around H_{eff} . The second term with first-order time derivative of \vec{M} , is the Gilbert damping term [12], which occurs due to the transfer of energy and angular momentum of \vec{M} to the environmental degrees of freedom (relaxation of \vec{M} towards \vec{H}_{eff}).

Figure 4(a) shows the representative Kerr rotation data of Py (5 nm) sample for $F = 4.6 \text{ mJ cm}^{-2}$ and $\mu_0 H = 113 \text{ mT}$ consisting of three temporal regions, i.e., ultrafast demagnetization, fast remagnetization, and slow remagnetization superposed with damped precession within the time window of 900 ps. The slower remagnetization is mainly due to heat diffusion from the lattice to the substrate and the surroundings. Figure 4(b) shows the background subtracted time-resolved Kerr rotation data (precessional part) for two different values of the external field H_{ext} , fitted with a damped sinusoidal function,

$$M(t) = M(0)e^{-t/\tau_d} \sin(2\pi ft) \quad (3)$$

Here, $M(0)$ is the initial amplitude of precession, τ_d is the relaxation time of the coherent precession obtained as a fitting parameter, and f is the precessional frequency, which can also be extracted directly from the fast Fourier transform (FFT) of the precessional oscillation. Due to the size of the laser spot, our measurement detects in very good approximation only the uniform precession of the magnetization, the Ferromagnetic Resonance (FMR), which is equivalent to a magnon with vanishing wave vector. The effective magnetization (M_{eff}), which includes the saturation magnetization and potential additional out-of-plane anisotropies, is calculated from the H dependence of the FMR frequency (Fig. 4(c)) and fitting the data points with the Kittel formula [20],

$$f = \frac{\gamma}{2\pi} \sqrt{(H_{\text{ext}} + H_k)(H_{\text{ext}} + H_k + 4\pi M_{\text{eff}})} \text{ (cgs)} \quad (4)$$

where $\gamma = 1.83 \times 10^7 \text{ Hz Oe}^{-1}$ for Py. Strictly speaking, Eqn. 4 is only valid for an completely in-plane magnetized film, but we have verified using micromagnetic simulations that it approximates our experimental situation very well. From the fit, M_{eff} is obtained to be $\sim 700 \pm 25 \text{ kA m}^{-1}$ for 5 nm Py [and $\sim 670 \pm 20 \text{ kA m}^{-1}$ for 2.8 nm Py as shown in the supplemental materials] measured at a pump fluence (F) of 4.6 mJ cm^{-2} . If one studies the excitation of the coherent magnons, a first interesting point is the dependence of the precession amplitude on the external conditions. As (Fig. 4(d)) shows, the precessional amplitude for a fixed pump fluence of

Interestingly, we observe that the precessional relaxation time (τ_d) as obtained from TR-MOKE measurements, increases with increase of H_{ext} (Fig. 4(e) red dots), which is unexpected if one assumes that Gilbert damping is responsible for the decay of the precession. Since Gilbert damping is viscous, it predicts a decrease of the magnon lifetime with increasing frequency, which is equivalent to an increase in magnetic field strength in the presented geometry. This is also clearly reflected by independent measurements of the FMR lifetime using inductive microwave measurements by microwave spectroscopy using a vector-network analyzer (Fig. 4(e) blue dots). Likewise, analytical calculations of the

magnon characteristics based on the Gilbert model [21]–[24] show the same behavior of the Gilbert-induced lifetime, decreasing with increasing external magnetic field. For these analytical calculations, we assumed an in-plane field but we verified again using micromagnetic simulations that the

This is because both incoherent and coherent magnons are excited when the sample is hit with a fs laser pulse in TR-MOKE.

This is in contrast to FMR measurements where we mainly study coherent magnons (no thermally excited incoherent magnons are present). Thus, in the case of TR-MOKE measurements, the possibility of two-magnon scattering or multi-magnon scattering leads to such an increase of τ_d with H . This is because with decreasing H the probability of excitation of incoherent magnons in ultrathin films increases compared to coherent magnons, leading to lower τ_d at lower H . The data for the 2.8 nm Py sample show similar trends and are provided in the supplementary materials.

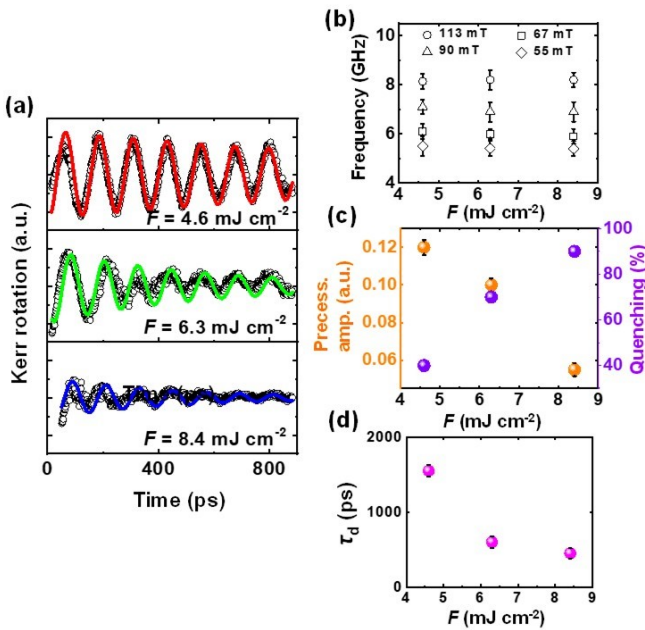


Fig. 5. Fluence (F) dependent dynamics: (a) Background-subtracted time-resolved Kerr rotation data for 5 nm Py sample measured at $H = 113$ mT and different pump fluence (F). Solid lines are fitting lines. (b) F dependence of precessional frequencies at different H . (c) F dependence of percentage quenching (lilac) and precessional amplitude (yellow). (d) F dependence of precessional relaxation time (τ_d).

The background subtracted time-resolved Kerr rotation data for the 5 nm Py sample measured at different pump fluences (F) are shown in Fig. 5(a). The energy deposited by the pump pulse, in terms of heat within the probed volume, plays a very crucial role in modification of local magnetic properties, i.e., magnetic moment, anisotropy, coercivity, magnetic susceptibility, etc. as well as the precessional frequency may experience a variation with pump fluence [5], [25]. However, we do not observe any such significant frequency shift within our experimental fluence range as shown in Fig. 5(b). Also, M_{eff} does not show any significant fluence dependence within our experimental fluence range (see supplemental materials).

Thus, we infer that with increasing fluence, there is no induced anisotropy developing in the system that can modify the effective magnetization up to this extent [26]. The dependence of the precessional relaxation time (τ_d) with pump fluence (F) shows a decrease of τ_d with F (Fig. 5(d)). This is again explained by the dephasing due to nonlinear magnon interactions and the incoherent magnon background, as probability of excitation of incoherent magnons as compared to coherent magnons become more at higher F . Also, with increasing pump fluence, the ratio between system temperature and Curie temperature (T/T_C) increases due to the heating effect from the pump laser irradiation. As a consequence, τ_d decreases which fundamentally depends on susceptibility, as predicted theoretically [5], [26], [27].

For the IP configuration, we observe a reduction in precessional amplitude leading to a poor signal-to-noise ratio (see supplemental materials). As the magnetic field is tilted slightly ($\sim 15^\circ$) in the OOP direction, the precessional amplitude increases and we observe a clear time-resolved Kerr rotation trace resulting clear fast Fourier transformed magnon modes. In the IP configuration the dominance of nonmagnetic noise has suppressed the features of magnetic peaks and only a few spurious peaks are present in the spectra.

IV. SUMMARY

In summary, using an all-optical TR-MOKE technique, the spin dynamics on different timescales in ultrathin $\text{Ni}_{80}\text{Fe}_{20}$ films have been investigated. We study the precessional dynamics in the GHz range followed by femtosecond laser induced ultrafast demagnetization for our samples. The demagnetization time, fast remagnetization time, and magnetization quenching in our samples exhibit an increasing trend with excitation fluence, consistent with a spin-flip scattering-dominated demagnetization process. In the precessional regime, magnetic field and pump fluence dependence of several important parameters (e.g. effective magnetization, precessional relaxation time etc.) have been thoroughly discussed. We observe an unusual variation of the precessional relaxation time in TR-MOKE measurements, which can be related to the magnon-magnon interactions along with incoherent magnon background after excitation with a fs laser pulse. We envisage that our results will shed light to future experimental and theoretical investigations toward a deeper understanding of spin dynamics over a broad timescale.

V. ACKNOWLEDGEMENT

The authors acknowledge Eva Prinz, Jonas Hofer, and Martin Stehil for support during the experiment. The work has been funded by the Deutsche Forschungsgemeinschaft (DFG, German Research Foundation) through No. TRR 173-268565370 Spin + X: spin in its collective environment (Project B11).

REFERENCES

- [1] M. van Kampen, C. Jozsa, J. T. Kohlhepp, P. LeClair, L. Lagae, W. J. M. de Jonge, and B. Koopmans, “All-optical probe of coherent spin waves,” *Phys. Rev. Lett.*, vol. 88, p. 227201, May 2002. [Online]. Available: <https://link.aps.org/doi/10.1103/PhysRevLett.88.227201>

- [2] A. Barman and J. Sinha, "Spin dynamics and damping in ferromagnetic thin films and nanostructures," 2017.
- [3] E. Beaurepaire, J.-C. Merle, A. Daunois, and J.-Y. Bigot, "Ultrafast spin dynamics in ferromagnetic nickel," *Phys. Rev. Lett.*, vol. 76, pp. 4250–4253, May 1996. [Online]. Available: <https://link.aps.org/doi/10.1103/PhysRevLett.76.4250>
- [4] M. D. Kaufmann, "Magnetization dynamics in all-optical pump-probe experiments: spin-wave modes and spin-current damping," 2006.
- [5] S. Mondal and A. Barman, "Laser controlled spin dynamics of ferromagnetic thin film from femtosecond to nanosecond timescale," *Phys. Rev. Appl.*, vol. 10, p. 054037, Nov 2018. [Online]. Available: <https://link.aps.org/doi/10.1103/PhysRevApplied.10.054037>
- [6] B. Koopmans, J. J. M. Ruigrok, F. D. Longa, and W. J. M. de Jonge, "Unifying ultrafast magnetization dynamics," *Phys. Rev. Lett.*, vol. 95, p. 267207, Dec 2005. [Online]. Available: <https://link.aps.org/doi/10.1103/PhysRevLett.95.267207>
- [7] J. Walowski, G. Müller, M. Djordjevic, M. Münzenberg, M. Kläui, C. A. F. Vaz, and J. A. C. Bland, "Energy equilibration processes of electrons, magnons, and phonons at the femtosecond time scale," *Phys. Rev. Lett.*, vol. 101, p. 237401, Dec 2008. [Online]. Available: <https://link.aps.org/doi/10.1103/PhysRevLett.101.237401>
- [8] M. Djordjevic, G. Eilers, A. Parge, M. Münzenberg, and J. S. Moodera, "Intrinsic and nonlocal gilbert damping parameter in all optical pump-probe experiments," *Journal of Applied Physics*, vol. 99, no. 8, p. 08F308, 2006. [Online]. Available: <https://doi.org/10.1063/1.2177141>
- [9] S. Mukhopadhyay, S. Majumder, S. N. Panda, and A. Barman, "Investigation of ultrafast demagnetization and gilbert damping and their correlation in different ferromagnetic thin films grown under identical conditions," 2023.
- [10] A. Barman, S. Wang, J. D. Maas, A. R. Hawkins, S. Kwon, A. Liddle, J. Bokor, and H. Schmidt, "Magneto-optical observation of picosecond dynamics of single nanomagnets," *Nano Letters*, vol. 6, no. 12, pp. 2939–2944, 2006, pMID: 17163735. [Online]. Available: <https://doi.org/10.1021/nl0623457>
- [11] R. Wilks, R. J. Hicken, M. Ali, B. J. Hickey, J. D. R. Buchanan, A. T. G. Pym, and B. K. Tanner, "Investigation of ultrafast demagnetization and cubic optical nonlinearity of ni in the polar geometry," *Journal of Applied Physics*, vol. 95, no. 11, pp. 7441–7443, 2004.
- [12] T. Gilbert, "A phenomenological theory of damping in ferromagnetic materials," *IEEE Transactions on Magnetics*, vol. 40, no. 6, pp. 3443–3449, 2004.
- [13] E. Carpene, E. Mancini, C. Dallera, M. Brenna, E. Puppini, and S. De Silvestri, "Dynamics of electron-magnon interaction and ultrafast demagnetization in thin iron films," *Phys. Rev. B*, vol. 78, p. 174422, Nov 2008. [Online]. Available: <https://link.aps.org/doi/10.1103/PhysRevB.78.174422>
- [14] F. Dalla Longa, J. T. Kohlhepp, W. J. M. de Jonge, and B. Koopmans, "Influence of photon angular momentum on ultrafast demagnetization in nickel," *Phys. Rev. B*, vol. 75, p. 224431, Jun 2007. [Online]. Available: <https://link.aps.org/doi/10.1103/PhysRevB.75.224431>
- [15] B. Koopmans, G. Malinowski, F. Dalla Longa, D. Steiauf, M. Fähnle, T. Roth, M. Cinchetti, and M. Aeschlimann, "Explaining the paradoxical diversity of ultrafast laser-induced demagnetization," *Nat. Mater.*, vol. 9, p. 259–265, 2010.
- [16] T. Roth, A. J. Schellekens, S. Alebrand, O. Schmitt, D. Steil, B. Koopmans, M. Cinchetti, and M. Aeschlimann, "Temperature dependence of laser-induced demagnetization in ni: A key for identifying the underlying mechanism," *Phys. Rev. X*, vol. 2, p. 021006, May 2012. [Online]. Available: <https://link.aps.org/doi/10.1103/PhysRevX.2.021006>
- [17] M. Krauß, T. Roth, S. Alebrand, D. Steil, M. Cinchetti, M. Aeschlimann, and H. C. Schneider, "Ultrafast demagnetization of ferromagnetic transition metals: The role of the coulomb interaction," *Phys. Rev. B*, vol. 80, p. 180407, Nov 2009. [Online]. Available: <https://link.aps.org/doi/10.1103/PhysRevB.80.180407>
- [18] M. Cinchetti, M. Sánchez Albaneda, D. Hoffmann, T. Roth, J.-P. Wüstenberg, M. Krauß, O. Andreyev, H. C. Schneider, M. Bauer, and M. Aeschlimann, "Spin-flip processes and ultrafast magnetization dynamics in co: Unifying the microscopic and macroscopic view of femtosecond magnetism," *Phys. Rev. Lett.*, vol. 97, p. 177201, Oct 2006. [Online]. Available: <https://link.aps.org/doi/10.1103/PhysRevLett.97.177201>
- [19] S. Eich, M. Plötzing, M. Rollinger, S. Emmerich, R. Adam, C. Chen, H. C. Kapteyn, M. M. Murnane, L. Plucinski, D. Steil, B. Stadtmüller, M. Cinchetti, M. Aeschlimann, C. M. Schneider, and S. Mathias, "Band structure evolution during the ultrafast ferromagnetic-paramagnetic phase transition in cobalt," *Science Advances*, vol. 3, no. 3, p. e1602094, 2017.
- [20] C. Kittel, "On the theory of ferromagnetic resonance absorption," *Phys. Rev.*, vol. 73, pp. 155–161, Jan 1948. [Online]. Available: <https://link.aps.org/doi/10.1103/PhysRev.73.155>
- [21] B. Kalinikos, "Excitation of propagating spin waves in ferromagnetic films," *IEE Proceedings H Microwaves, Optics and Antennas*, vol. 127, no. 1, p. 4, 1980.
- [22] B. A. Kalinikos and A. N. Slavin, "Theory of dipole-exchange spin wave spectrum for ferromagnetic films with mixed exchange boundary conditions," *Journal of Physics C: Solid State Physics*, vol. 19, no. 35, p. 7013, dec 1986.
- [23] B. A. Kalinikos, M. P. Kostylev, N. V. Kozhus, and A. N. Slavin, "The dipole-exchange spin wave spectrum for anisotropic ferromagnetic films with mixed exchange boundary conditions," *Journal of Physics: Condensed Matter*, vol. 2, no. 49, p. 9861, dec 1990.
- [24] D. D. Stancil and A. Prabhakar, *Quantum Theory of Spin Waves*. Boston, MA: Springer US, 2009, pp. 33–66.
- [25] S. Mizukami, H. Abe, D. Watanabe, M. Oogane, Y. Ando, and T. Miyazaki, "Gilbert damping for various ni80fe20 thin films investigated using all-optical pump-probe detection and ferromagnetic resonance," *Applied Physics Express*, vol. 1, no. 12, p. 121301, nov 2008. [Online]. Available: <https://dx.doi.org/10.1143/APEX.1.121301>
- [26] B. Liu, X. Ruan, Z. Wu, H. Tu, J. Du, J. Wu, X. Lu, L. He, R. Zhang, and Y. Xu, "Transient enhancement of magnetization damping in cofeb film via pulsed laser excitation," *Applied Physics Letters*, vol. 109, no. 4, p. 042401, 2016.
- [27] P. Nieves, D. Serantes, U. Atxitia, and O. Chubykalo-Fesenko, "Quantum landau-lifshitz-bloch equation and its comparison in the classical case," *Phys. Rev. B*, vol. 90, p. 104428, Sep 2014. [Online]. Available: <https://link.aps.org/doi/10.1103/PhysRevB.90.104428>